

# The PEGASES gridded ion-ion thruster performance and predictions

IEPC-2013-259

*Presented at the 33rd International Electric Propulsion Conference,  
The George Washington University • Washington, D.C. • USA  
October 6 – 10, 2013*

A. Aanesland<sup>1</sup>, D. Rafalskyi, J. Bredin, P Grondein, N. Oudini<sup>2</sup>, and P. Chabert  
*Laboratoire de Physique des Plasmas (LPP), CNRS-Ecole Polytechnique, 91128 Palaiseau Cedex, France*

L. Garrigues, G. Hagelaar  
*Laboratoire PLAsma et Conversion d'Energie - LAPLACE, 31062 Toulouse Cedex 9, France*

**Abstract:** The PEGASES (Plasma propulsion with Electronegative gases) thruster is a gridded ion thruster that accelerates alternately positively and negatively charged ions to provide thrust. Over the last years various prototypes have been tested, adequate diagnostics have been developed and analytical models and simulations are made to better understand and control the physics involved. We have recently provided the first experimental proof-of-concept, accelerating alternately positive and negative ions from an ion-ion plasma within a 10 kHz cycle. The plasma density and ion current in the region of the ion-ion plasma predicts that the performance of the PEGASES thruster can be comparable to existing thrusters on the market with currently a prediction of  $17 \text{ mN.kW}^{-1}.\text{kV}^{-1}$  thrust. Here we present the state of the art in the PEGASES development and discuss its possible future in space.

## Nomenclature

$\alpha = n_-/n_e$	=	Electronegativity
$n_{+,-,e}$	=	Positive (+), negative (-) and electron (e) density
$T_{+,-,e}$	=	Positive (+), negative (-) and electron (e) temperature
$v_{ex}, v_b, u_B$	=	Exhaust (ex), ion beam (b) and Bohm (B) velocity
$\Gamma$	=	Particle flux
PTE	=	Power Transfer Efficiency
ICP	=	Inductively Coupled Plasma
PIC	=	Particle In Cell

## I. Introduction

IN contrast to classical gridded thrusters, the PEGASES thruster generates thrust by accelerating both positive and negative ions from the same source<sup>1</sup>. This system therefore provides thrust without the need for additional current and space charge neutralization, it will provide a downstream beam or plume mostly composed of fast neutrals with a low density of charged particles, and it will allow the control of the net charge out of the thruster and hence the charging of the satellite/space probe can be controlled. These qualities make the PEGASES an attractive technology for various classical space applications (attitude control or deep space missions), but also for more sophisticated concepts such as the Ion Beam Shepherd for Contactless Space Debris Removal.<sup>2</sup>

For the sake of simplicity, the thruster can be divided into four regions:

<sup>1</sup> ane.aanesland@lpp.polytechnique.fr

<sup>2</sup> now at Istituto di Metodologie Inorganiche e dei Plasmi, CNR, via Amendola 122/D, 70126 Bari, Italy

- i) The ferrite enhance ICP source for plasma generation,
- ii) The magnetic barrier region for ion-ion plasma formation,
- iii) The extraction and acceleration region to generate thrust and
- iv) The downstream space charge neutralization and recombination region to generate the desired beam/plume performance.

To a first approximation these regions are, as for classical gridded ion thrusters, not directly connected, allowing each part to be investigated separately. Here we will take a look at the current state of performance and physical understanding within these four regions of the thruster and we will discuss the link between the transport processes within the plasma and the possible extraction of ions, in particular the negative ions. The paper is organized as follows. In section II the PEGASES II prototype and source operating conditions are described, in section III densities of ions and electrons are presented together with the ratio  $\alpha$  (describing the electronegativity) showing that high-density ion-ion plasmas are generated in front of the acceleration grids. Section IV presents the experimental results of alternate acceleration of positive and negative ions together with some link to particle-in-cell simulations. Section V presents a preliminary estimate of the PEGASES thruster performance, and a conclusion is drawn in section VI.

## II. PEGASES II prototype

The PEGASES second prototype is shown schematically on figure 1. The source volume is rectangular with a cross section of 10 by 8 cm and a length of 12 cm.<sup>3,4</sup> The plasma is generated by a pure inductively coupled source at 4 MHz. The RF power is coupled to the plasma via a planar inductor separated from the plasma via a thin ceramic window. The inductor coil is driven symmetrically via an impedance matching network consisting of a low loss transmission-line transformer and air variable capacitors in symmetrical (push-pull) configuration. This increases the current in the coil and reduces the voltage, such that capacitive coupling effects are eliminated. The inductive coil is further embedded in a ferrite for enhanced power efficiency. The technology of efficient ICP sources is described in detail in Godyak *et al.*<sup>5</sup>

The gas is injected along the source axis via 16 small holes distributed on both sides of the source. In the current laboratory experiments we use Argon and/or SF<sub>6</sub>. Permanent magnets are used to generate a localized magnetic barrier perpendicular to the extraction/acceleration axis. The configuration of this field is discussed below, briefly it is a Gaussian magnetic field with the maximum of 245 G placed 7.5 cm from the ceramic window.

Currently three copies of this prototype are installed on various test-bed experiments (two at LPP and one at ICARE<sup>6</sup>). For a thorough investigation of the plasma inside the thruster, one copy is mounted on a relatively small vacuum chamber to avoid volume expansion at the exit of the source. This prototype has conducting walls such that Langmuir probes can be used without the risk of large perturbation from lack of return current to the walls. The analysis of the Langmuir probe data is detailed in Bredin *et al.* and provides densities and temperatures of both ions and electrons in strongly electronegative plasmas.<sup>4</sup>

For the experiments on alternate ion acceleration the walls in contact with the plasma is of Pyrex (as shown on figure 1) and the thruster is attached to a large vacuum chamber where the pressure in the thruster under operation is 10-50 times higher than in the downstream chamber. A set of grids are placed 12 cm from the ceramic window. The two grids are separated by 2 mm with 2.5 mm diameter holes. The optical transparency of each grid is 60%. A cylindrical Langmuir probe and a planar ion flux probe are inserted through the grids and are used to measure plasma parameters in the vicinity of the extraction grids. A Magnetized Retarding Field Energy Analyzer (MRFEA) is placed in the downstream chamber to measure both positive and negative ion energies. This analyzer is still under development but the principle can be found in Rafalskyi *et al.*<sup>7</sup>

### A. Source operating conditions

The RF power and gas pressure controls the source efficiency. In this prototype the frequency is fixed at 4 MHz, but varying this frequency could also contribute to increased efficiency.

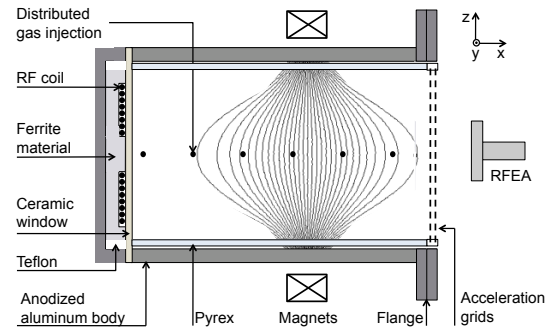


**Figure 1 Schematic of the PEGASES II prototype.**

The plasma density increases linearly with the RF power, as in standard ICP sources<sup>5</sup>. We therefore use 200 W in most experiments (unless stated otherwise) as this provides high plasma density with reduced complication with heating of the ICP source etc. Figure 2a and b shows the power transfer efficiency and the measured ion current density as a function of pressure in pure Argon and SF<sub>6</sub>. The power transfer efficiency (PTE) reaches a maximum at 0.7-1 mTorr for SF<sub>6</sub> (where PTE is 50%) while it increases with pressure in argon. PTE is higher in Argon than in SF<sub>6</sub> and reflect a change in the plasma impedance that might be due to dissociation processes in SF<sub>6</sub> (these processes increase with pressure as seen on the evolution of PTE). The ion current density at the position of the grids is largest for 0.7-1 mTorr. The discharge in SF<sub>6</sub> cannot be sustained below 0.7 mTorr and above 3 mTorr for the power and magnetic field used. The typical total pressure used in our experiments is therefore 1 mTorr. This insures a safe operation of the source without the risk of the discharge vanishing under investigation.

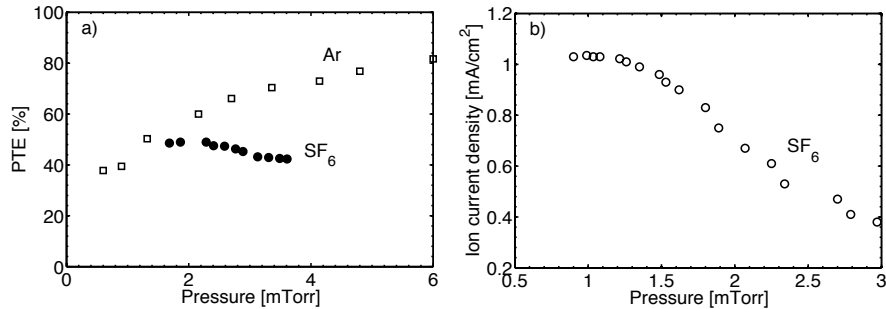


Figure 2 a) Power Transfer Efficiency (PTE) in Argon (squares) and SF<sub>6</sub> (circles) and b) Ion current density towards the grid as a function of pressure.

### III. Ion-Ion plasma

The parameters determining the formation of an ion-ion plasma region downstream of the magnetic filter are naturally the strength of the magnetic field and the location of its maximum position. We will see below that also the gas mixture plays a role in this ion-ion formation.

Figure 3 a) shows the ion and electron density along the axis of the thruster operating in SF<sub>6</sub> from the ceramic window at  $x=0$  cm to the exit of the thruster at 14 cm. In this case no grids are placed at the extraction surface. Figure b) shows the ratio between the negative ion density and the electron density. This ratio called  $\alpha$  is typically used to describe electronegative plasmas. From 0 to 4 cm, the electron density is fairly constant (this corresponds to the heating region by the radio-frequency electromagnetic field localized in the skin depth in the first few centimeters away from the dielectric window), and drops by two orders of magnitude between 5 cm and 8.5 cm. In the heating region, the electronegativity is modest,  $\alpha \approx 5$ , but it drastically increases in the magnetic barrier region to reach  $\alpha \sim 2000$  at 9 to 15 cm. The ion densities decay slowly due to surface wall losses and volume recombination. The negative ion dominates the current carried by negative charges to the walls, probes or electrodes when  $\alpha > 500$ .<sup>7</sup> At this value of  $\alpha$  one can consider that an ion-ion plasma is formed, which is obtained here around 8 cm.

The position of ion-ion formation changes with the position of the magnetic field (i.e. the magnets), and we have found that the optimal position is at 7.5 cm from the ceramic window (i.e. from the induction coil that generates the plasma) with a maximum strength of 245 G on axis.<sup>4</sup> This allows a stable operation of the ICP source, with reduced coupling between the inductive field from the RF coil and the DC magnetic field.

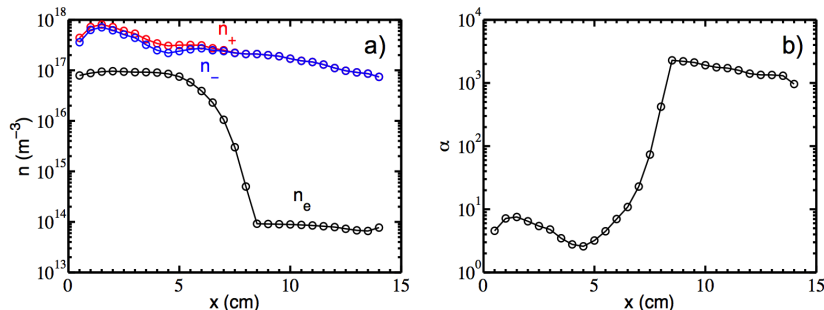
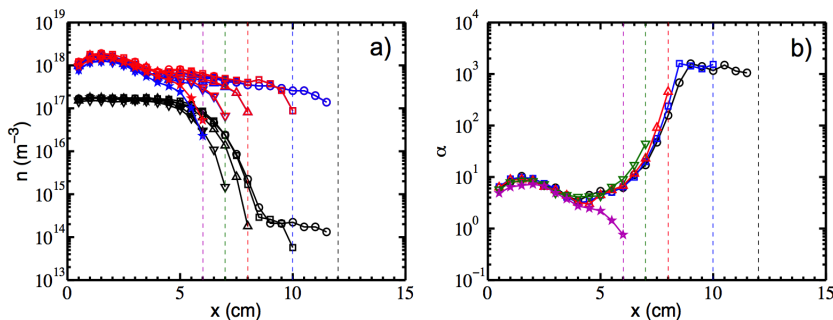


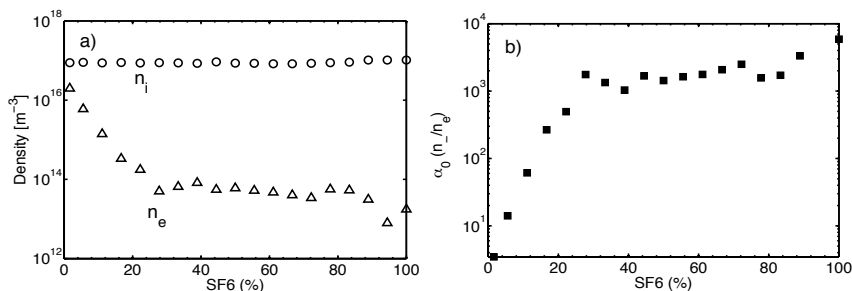
Figure 3 a) Positive and negative ion and electron densities and b) the electronegativity ( $\alpha=n_-/n_e$ ) as a function of axial position from the ceramic window at  $x=0$ . The maximum magnetic field is at 7.5 cm.

Figure 4 a) and b) shows the ion and electron densities and electronegativity  $\alpha$  as a function of the axial position when a floating grid is installed. The five sets of experiments correspond to the grid position downstream of the magnetic barrier and the position is indicated by the dashed lines in the figures. The grid position has little influence on the formation of the ion-ion plasma, as long as the grids are placed downstream of the maximum magnetic field. The negative ion density in front of the grid does not change much between the grid position of 8 and 10 cm. The electron density and the ratio  $\alpha$  therefore indicated that the best position for the acceleration grids is at 10 cm from the ceramic window. At this position the ion density is  $2 \times 10^{17} \text{ m}^{-3}$  for only 200 W input RF power (i.e. total power coming from the generator).



**Figure 4 a) Negative ion and electron density and b)  $\alpha$  as a function of axial position for various positions of the acceleration grids. The grids are here floating.**

An electronegative gas is required in the PEGASES thruster such that both ionization and dissociate attachment, creating respectively positive and negative ions occurs. Electronegative gases are molecular halogen-containing gases, and as seen on figure 2a the power transfer efficiency is not as high as for inert gases, and much of the discharge power goes to neutral dissociation processes. In the current laboratory experiments we use mixtures of Argon and  $\text{SF}_6$ . Figure 5 shows that only 20% of  $\text{SF}_6$  is required to form an ion-ion plasma downstream of the magnetic filter. This means that we can reduce the amount of electronegative gas and hence reduce the loss in dissociation and also reduce and control etching and deposition problems seen in these types of plasmas. Although here we are using  $\text{SF}_6$  as the electronegative gas, a PEGASES thruster in space would probably be best operated with Iodine or gas mixtures of an inert gas (Xenon or Argon) together with Iodine.



**Figure 5 a) Ion and electron density and b) the electronegativity  $\alpha$  as a function of the percentage of  $\text{SF}_6$  in an Argon discharge. The pressure is kept at 1 mTorr, and the probe is placed 10 cm from the ceramic window.**

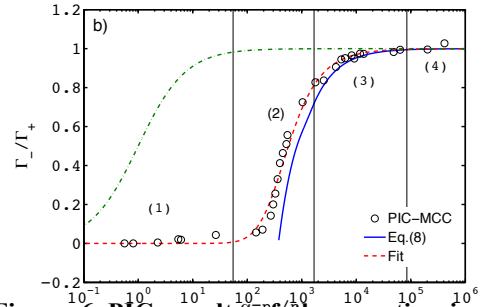
#### IV. Alternate acceleration of positive and negative ions

The PEGASES thruster is a gridded ion thruster based on classical gridded acceleration. However, as described briefly in the introduction, the first grid in contact with the plasma is biased with a square or sinusoidal voltage waveform. The electric field between the grids will therefore change direction and accelerate positive and negative ions in the respective bias periods. In order for this acceleration concept to work, the potential of the plasma needs to follow the grid potential and allow both fluxes of positive and negative ions to reach the grids. The first criterion is met by isolating the plasma from the grounded walls, in this case by using Pyrex walls, such that the reference potential is given by the first grid in contact with the plasma. The latter condition is met by the formation of an ion-

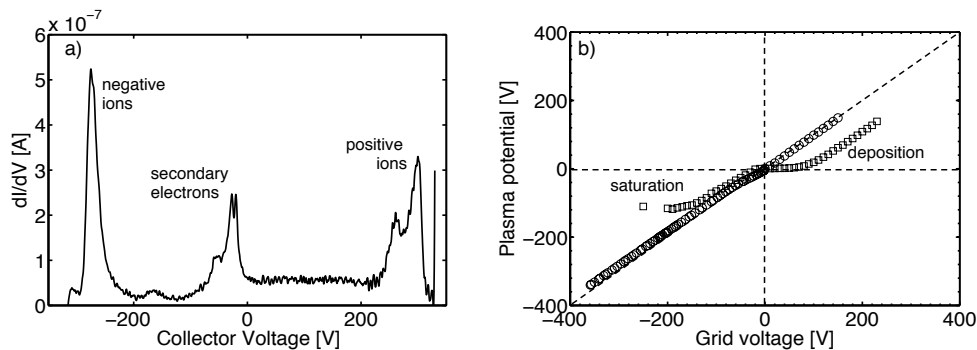
ion plasma in front of the grids. Figure 6 shows results from a 1D PIC simulation where the ion flux ratio is obtained as a function of the electronegativity  $\alpha$ .<sup>8</sup> We show here that electronegative plasmas can be divided into four regimes. At low  $\alpha$  (regime 1) negative ions are confined in the plasma due to the ambipolar electric field created by the mobile electrons. With increasing  $\alpha$ , the flux of negative ions towards the walls increases and at  $\alpha > 2000$  the flux equals the flux of positive ions. At this high electronegativity, PIC simulations show further that fluxes of positive and negative ions can be alternately extracted from the plasma using biased electrodes.<sup>9</sup>

Figure 7a shows the ion energy distribution function measured when a square waveform at a voltage of  $\pm 300$  V and a frequency of 30 KHz is applied to the first grid. The two large peaks correspond to a negative and a positive ion beam and the low energy peak for negative charges correspond to secondary electrons created in the analyzer and electrons created in the downstream region. This distribution function is measured continuously and hence represents the beam after many bias periods. However time resolved measurements show that the positive and negative ions are accelerated in packets within the respective bias periods and have constant peak amplitude and beam energy.

Figure 7b shows the plasma potential in the thruster as a function of the grid voltage for two operation conditions. The square symbols shows the plasma potential measured in conditions where a dielectric film is formed on the grid.<sup>10</sup> This film strongly influence the positive ion energies as some of the voltage is dropped in the dielectric layer on the grid; as a result the effective acceleration voltage is reduced. This has been confirmed by measuring the ion beam energies (i.e. the position of the measured ion peaks in figure 7a). The negative plasma biasing is not strongly influenced by this dielectric film due to a particular film destruction.<sup>9</sup> The negative plasma potential saturates and as a result the negative ion flow disappears at larger negative potentials ( $< -150$  V). This can be explained as follows. When the plasma is polarized strongly negative the plasma electrons leak to ground via the small apertures in the gas injection system. Hence, preventing the plasma potential to be further negative, i.e. the plasma potential saturates. At sufficient negative potential, the sheath in front of the grids becomes space charge positive and negative ions can not any longer be extracted from the plasma and negative ion beams are not detected in the downstream region. This is equivalent to a system in regime 1 of figure 6. The circles in figure 7b are obtained at higher bias frequencies, which prevent the dielectric film to form on the grids, hence the positive ion beam energy correspond to the applied bias potential. The leakage paths to grounds are also fixed such that the plasma can be negatively polarized allowing acceleration of negative ions. Beams of  $\pm 400$  V have been measured. The positive and negative ion masses are not yet specified, and since the grids are far from optimized the beam currents are still rather low.



**Figure 6 PIC results of the negative ion to positive ion flux ratio towards the electrode as a function of the electronegativity.<sup>8</sup>**



**Figure 7 MRFEA measuring negative and positive ion beams and b) plasma potential as a function of the grid voltage for a situation with dielectric deposition (squares) and without deposition and leakage currents (circles).**

## V. Performance estimation

Since the acceleration optics is not optimized for the current plasma conditions, we will here make an estimate of the performance by the measured ion flux (figure 2b) as well as the densities and temperatures (figure 4a) in front of

the grids, as these values are more precise. We therefore assume in the following estimate that the grids are performing as conventional gridded thrusters on the market today.

The thrust from a gridded thruster can be expressed as

$$T = -\frac{dm}{dt}v_{ex} = A_i\Gamma_iM_iv_b, \quad (1)$$

where  $A_i$  is the effective acceleration surface,  $\Gamma_i$  is the flux of ions from the plasma,  $M_i$  is the ion mass, and  $v_b$  is the ion beam velocity. The ion flux from the plasma is given by the ion density  $n_i$  and the ion Bohm speed  $u_B$  where  $u_B = \sqrt{kT_e/M_i}$  in classical electropositive plasmas. In the case of pure ion-ion plasma it has been shown that the ions enter the sheath with an equivalent Bohm speed, where the electron temperature is replaced by the ion temperature of the ions that are reflected from the boundary. Hence, in a gridded thruster the thrust can be rewritten as

$$T = A_ien_s\sqrt{2T_{e,i}V_{accel}}, \quad (2)$$

where  $n_s$  is the ion density at the sheath edge,  $T_{e,i}$  is the electron or ion temperature and  $V_{accel}$  is the effective acceleration voltage. The thrust efficiency is given by

$$\eta_T = \frac{T^2}{2Q_{total}P_{in}}, \quad (3)$$

where  $Q_{total}$  is the total mass flow rate and  $P_{in}$  is the total power used.

We also define the normalized thrust as  $\xi = T/(P_{in}V_{accel})$ . Table I shows the numbers for PEGASES together with a comparison with the T6 gridded thruster from QinetiQ<sup>10</sup>.

Performance estimations		
	PEGASES	T6 <sup>10</sup>
$n_i$	$2.0 \times 10^{11} \text{ cm}^{-3}$	$2.2 \times 10^{11} \text{ cm}^{-3}$
$T_{e,i}$	0.2 eV	6.0 eV
$J_b$	1 mA/cm <sup>2</sup>	5.8 mA/cm <sup>2</sup>
$A_i$	96 cm <sup>2</sup>	380 cm <sup>2</sup>
$Q_{total}$	6 sccm = 0.57 mg/s	35.3 sccm (with neutralizer)
$V_{accel}$	1000 V	1000 V
P	200 W + 500 W	500 W + 2200 W
T	5.5 mN	117 mN
$\xi$	17 mN.kW <sup>-1</sup> .kV <sup>-1</sup>	42 mN.kW <sup>-1</sup> .kV <sup>-1</sup>
$\eta_T$	33.2 %	63.6 %
Neutralizer	NO	Yes

## VI. Conclusion

The PEGASES thruster is a gridded ion thruster that accelerates alternately positive and negative ions for thrust. The current prototype provides a high ion-ion density in the vicinity of the grids, with a measured current density of 1 mA/cm<sup>2</sup> and an ion-ion density of  $2 \times 10^{11} \text{ cm}^{-3}$ . For the current extraction surface this values predicts a thrust of 5.5 mN. Experimental measurements show that positive and negative ions can be extracted from the thruster and accelerated to  $\pm 400\text{V}$  in cycles of 30 kHz without the need of an additional neutralizer system.

The PEGASES thruster needs an electronegative gas to be used to allow both ionization and dissociate attachment, creating respectively positive and negative ions. Electronegative gases are molecular gases containing Halogens. In the current laboratory experiments we use mixtures of Argon and SF<sub>6</sub>, and show that only 20% of this gas is required. A PEGASES thruster in space would probably be best operated with Iodine or gas mixtures of an inert gas (Xenon or Argon) together with Iodine. This allows tailoring the gas composition to reduce or completely avoid corrosive effects.

The current experiment on alternate acceleration is limited to frequencies in the kHz range. In laboratory experiments one can not exclude the contribution of secondary electrons formed in the downstream beam chamber and plays probably a role in the global neutralization/space charge compensation of the alternate beams. Analytical models, not shown here, predicts however that the frequencies of the alternate voltage waveform should be in the low MHz range, and opens for a simplified system where the plasma generation and ion acceleration can be achieved with the same power supply.

### Acknowledgments

This work is supported by EADS Astrium, by Agence Nationale de la Recherche under contract ANR- 2011-BS09-40 (EPIC) and by Marie Curie International Incoming Fellowship within the 7th European Community Framework (NEPTUNE- 326054).

### References

- <sup>1</sup>A. Aanesland, A. Meige, and P. Chabert, *J. Phys.: Conf. Ser.* **162**, 012009 (2009).
- <sup>2</sup>C. Bombardelli and J. Pelaez, *J. Guidance, Control and Dynamics.* **34**, 916–920 ( 2011).
- <sup>3</sup>A. Aanesland, J. Bredin, P. Chabert, V. Godyak, *Appl. Phys. Lett.* **100**, 044102 (2012).
- <sup>4</sup>J. Bredin, P. Chabert, and A. Aanesland, *Appl. Phys. Lett.*, **102**, 154107 (2013).
- <sup>5</sup>V. Godyak, *Plasma Sources Sci. Technol.* **20**, 025004 (2011).
- <sup>6</sup>D. Gerst, D. Renaud, S. Mazouffre, P. Chabert and A. Aanesland, *33rd International Electric Propulsion Conference*, Washington, DC, October 2013, paper *IEPC-2013-130*
- <sup>7</sup>D.V. Rafalskyi, S.V. Dudin, *Europhys. Lett.*, **97**, 55001 (2012)
- <sup>8</sup>N. Oudini, J.-L. Raimbault, P. Chabert, A. Meige and A. Aanesland, *Physics of Plasmas*, **20**, 043501 (2013).
- <sup>9</sup>N. Oudini, L. Garrigues, A. Meige, J.-L. Raimbault, P. Chabert and A. Aanesland, *Physics of Plasmas*, **19**, 103501 (2012).
- <sup>10</sup>D.V. Rafalskyi and S.V. Dudin, *Europhysics Letters*, **97**, 55001 (2012).